Atomistic Description of Reaction Intermediates in Supported Metathesis Catalysts Enabled by DNP SENS **

Ta-Chung Ong, Wei-Chih Liao, Victor Mougel, David Gajan, Anne Lesage, Lyndon Emsley, Christophe Copéret*

Abstract: Obtaining detailed structural information of reaction intermediates remains a key challenge in heterogeneous catalysis due to the amorphous nature of the support and/or the support interface that prohibits diffraction-based techniques. Here we use a combination of isotopic labeling and dynamic nuclear polarization (DNP) to increase the solid-state NMR signals of surface species in heterogeneous alkene metathesis catalysts. This in turn allows us to directly establish the bond connectivity and to measure carbon-carbon bond distance in trigonal bipyrimidal (TBP) and square pyramidal (SP) metallacycles, which are the cycloaddition intermediates in the alkene metathesis catalytic cycle. Furthermore, it made possible the understanding of the slow initiation and deactivation steps in well-defined heterogeneous metathesis catalysts.

Heterogeneous catalysts are key to efficient processes in the chemical industry. However, they are difficult to improve because of the lack of access to their active site structures, thus preventing rational approaches to designing better catalysts. Some of the most prominent examples are the Ziegler-Natta catalysts,[1] the Phillips polymerization catalysts,[2] and the alkene metathesis catalysts based on supported molybdenum, tungsten or rhenium oxides.[3] However, little is known about the active site structures of these industrial heterogeneous catalysts, and it is therefore not surprising that this field is still the focus of many debates and relies on empirical developments.[3-4] One approach to address this problem is surface organometallic chemistry, whose aim is to tailor the structures of active sites by controlled functionalization of surfaces.[5] As modern surface organometallic chemistry provides a means to generate specific active sites, it allows the possibility to determine structure–activity relationships and to implement rational strategies towards better catalyst designs. Even so, the method still faces the difficulty of obtaining structural information with the necessary level of detail, and which is today attainable for the homogeneous analogues. Consequently, active site structural information is usually acquired by indirect methods, such as comparison with models from molecular analogues.[6] Solution NMR spectroscopy has been particularly powerful in molecular catalysis to directly ascertain the structure and the dynamics of pre-catalysts or even to detect reaction intermediates.[7] NMR is sensitive to the local environment of the nuclei, and sophisticated multi-pulse and multi-dimensional experiments can be tailored to yield information about the electronic structure, the spatial arrangement, the environment, and the connectivity of given nuclei.[8] Today solid-state NMR can also provide a similar level of information for materials,[9] but the method is hindered by the intrinsically poor sensitivity of NMR combined with the fact that only a small fraction of the sample is of interest for surfaces. Therefore, there is a need to develop new approaches to gain access to NMR information of surface sites and reaction intermediates.

In the field of alkene metathesis, DFT studies have revealed that metallacyclobutanes are not only reaction intermediates, but that the trigonal bipyramidal (TBP) isomer is on the reaction pathway, and the square pyramidal (SP) isomer can be either a resting state of the catalyst or be involved in deactivation processes (Figure 1).[10] Experimentally, we previously observed that the more active catalyst **1** with a less σ-donating ligand (O^tBu_{F9}) generated mainly the TBP isomer and that, in contrast, the less active catalyst **2** with a more σ-donating ligand (O^tBu) generated mainly the SP isomer.[11] In molecular chemistry the structures of these two isomers were determined by X-ray crystallography,[12] but diffraction based techniques are not applicable because of the amorphous nature of supported catalysts, and the corresponding X-ray absorption techniques only provide an average structure of all surface species, e.g. isomers or other species. Recent studies were able to infer the presence of both TBP and SP intermediates in well-defined supported catalysts using solid-state NMR, albeit at the expense of long experiment times on fully ^{13}C labeled samples. This low sensitivity limited the studies only to the assignment of surface species by comparison with the known chemical shifts of the corresponding molecular species.[11, 13] Obtaining direct structural information, similar to that achieved on molecular species, e.g. C-C connectivity and bond distance measurements, would be a significant step forward in understanding surface site structures, but this step necessitates a major improvement in NMR sensitivity.

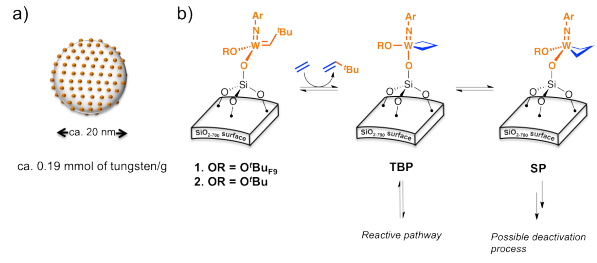

[*] Dr. T. C. Ong,[+] W.-C. Liao,[+] Dr. V. Mougel, Prof. Dr. C. Copéret
Department of Chemistry and Applied Biosciences, ETH Zürich, Vladimir Prelog Weg 1-5, 8093 Zürich, Switzerland
E-mail: ccoperet@ethz.ch
Dr. D. Gajan, Dr. A. Lesage, Prof. Dr. L. Emsley
Centre de RMN à Très Hauts Champs, Institut de Sciences Analytiques (CNRS/ENS Lyon/UCB Lyon 1), Université de Lyon, 69100 Villeurbanne, France
Prof. Dr. L. Emsley
Institut des Sciences et Ingénierie Chimiques, Ecole Polytechnique Fédérale de Lausanne (EPFL), 1015 Lausanne, Switzerland.
[+] These authors contributed equally
[**] DNP SENS = Dynamic Nuclear Polarization Surface Enhanced NMR Spectroscopy. We acknowledge the SNF for the 600 MHz DNP spectrometer (206021_150710) and funding for WCL (200020_149704). ERC Advanced Grant No. 320860 is acknowledged for funding support. Dr. René Verel, Prof. Dr. Aaron Rossini, Maxence Valla, and Dr. Daniel Silverio are acknowledged for many useful discussions. Dr. Aleix Comas-Vives and Dr. Francisco Núñez-Zarur are acknowledged for discussions regarding DFT calculations. Dr. Olivier Ouari and Prof. Dr. Paul Tordo are acknowledged for providing the TEKPol biradical. Lénaic Leroux is acknowledged for technical support at CRMN.

Supporting information for this article is given via a link at the end of the document.

Figure 1. a) Schematic representation of tungsten sites at the surface of SiO_2 nanoparticles and b) reaction of the tungsten alkylidene sites with ethylene to form the TBP and SP metallacyclobutane intermediates.

In recent years, dynamic nuclear polarization (DNP)[14] has made a major impact on the characterization of surface sites by improving the sensitivity of NMR by up to two orders of magnitude, thereby reducing the need for lengthy signal averaging and improving the detection limit.[15] The technique has the potential to contribute greatly to heterogeneous catalysis research.[16] It has been adapted and applied to the studies of a broad range of materials including hybrid materials,[15a, 15b, 15d] some particularly stable immobilized catalysts,[17] zeolites,[18] and nanoparticles,[15a, 15b, 15d, 19] However, it has yet to be used to probe the structure of reactive organometallic intermediates with atomic precision. In this report, we show that DNP surface enhanced NMR spectroscopy (DNP SENS), in combination with isotopic labeling, allows us to measure directly structural information of surface reaction intermediates in alkene metathesis catalysts, namely by obtaining C-C connectivities and bond distances of surface supported metallacyclobutane intermediates (Figure 1). The signal enhancement from DNP also allows us to observe the formation of initiation and deactivation products for the slower initiating catalyst, which involves a SP metallacycle intermediate.

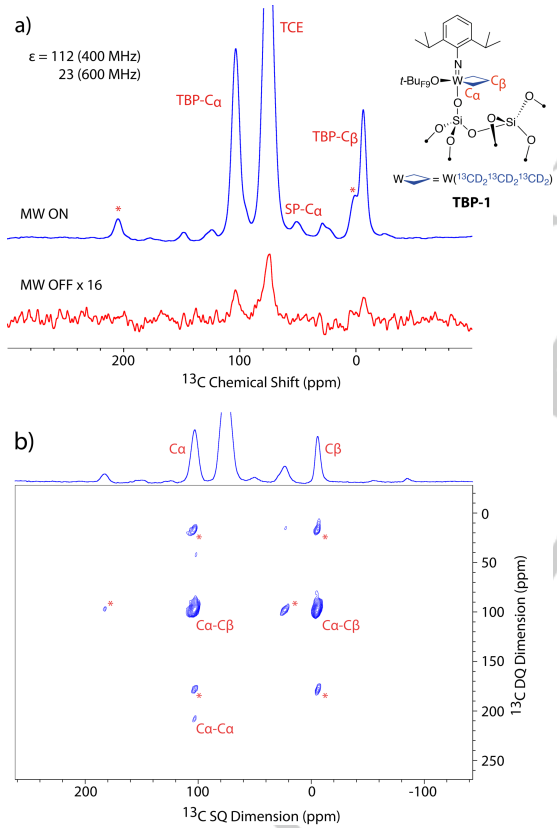

Figure 2. a) ^{13}C DNP SENS CPMAS spectra of ^{13}C and ^{2}H labeled tungsten TBP metallacycle (**TBP-1**), and b) two-dimensional DNP SENS refocused INADEQUATE of **TBP-1**, showing both the one-bond C_α-C_β and the two-bond C_α-C_α correlations. Both spectra were acquired with a 400 MHz DNP NMR spectrometer. Asterisks indicate spinning sidebands. Experimental parameters are given in SI.

Reaction of the catalyst **1** (≡SiO)W(NAr)(=CH*t*Bu)(O*t*Bu$_{F9}$)[11] with 10 equiv. of ^{13}C, ^{2}H labeled ethylene liberated 0.8 equiv. of 3,3-dimethyl-1-butene. After contacting the resulting solid with 16 mM TEKPOL[20] polarization agent in 1,1,2,2-tetrachloroethane (TCE) by incipient wetness impregnation, the sample was packed into a 3.2 mm sapphire rotor in an argon atmosphere glove box, and cooled to 100 K in the NMR probe. DNP SENS leads to signal enhancements of 23 and 112 for the sample at 600 MHz (14.1 T) and 400 MHz (9.4 T), respectively (Figure 2a). In the latter case, a S/N ratio of ca. 290 for the major surface species was obtained in only 80 seconds, while 15 hours were previously required to obtain a spectrum with much lower S/N ratio (90) on a 700 MHz (16.4 T) conventional spectrometer at room temperature.[11] The isotropic chemical shifts (δ_{iso}) of 102 ppm and –7 ppm are assigned to the C_α and C_β of a TBP metallacycle, **TBP-1** (Figure 2a).[11] The presence of the additional peak at 50 ppm is consistent with the C_α resonance of the associated SP metallacycle (**SP-1**) as a minor surface species.[11]

A DNP enhanced 2D refocused INADEQUATE[21] spectrum (Figure 2b) was recorded to corroborate the assignments. Since the INADEQUATE experiment (sequence shown in Figure S1) is a *J*-based correlation experiment, connectivity through chemical bond is required to excite double quantum (DQ) coherences. We were able to clearly observe the one-bond C_α-C_β correlation, as well as to detect the weaker two-bond C_α-C_α correlation. We also recorded a 2D POSTC7[22] experiment (sequence shown in Figure S2), which is a homonuclear dipolar recoupling sequence. As with the case of the refocused INADEQUATE spectrum, the C_α-C_β correlation of the TBP metallacycle was clearly observed, while the C_α-C_α correlation was absent (Figure S5). This absence is most likely due to the effect of dipolar truncation,[23] where the recoupling of the small C_α-C_α dipolar coupling is attenuated in the presence of the stronger C_α-C_β interaction. The presence of only the C_α-C_β dipolar correlation allows the distance between the two nuclei to be measured quantitatively via a series of 1D POSTC7 experiments with different mixing times.[24] Here the DQ efficiency was measured as a function of τ_{ex} by two different methods, the symmetric procedure and the constant time procedure.[24a, 24c] The resulting DQ efficiency curves (Figure S8) were simulated using SIMPSON[25] to calculate the C_α-C_β distance, which was found to be 1.54 (± 0.11) Å, in close agreement with the calculated C_α-C_β distance in a DFT optimized structure (1.59 Å) shown in Figure S3, and details are described in the Supporting Information.

Table 1. Experimental and calculated ^{13}C CSA parameters of the TBP metallacycle

	Condition	δ_{iso} (ppm)	Ω (ppm)	κ
C_α	100 K DNP	102.1 ± 6.7 (102.7)	180.9 ± 9.5 (194.5)	-0.99 ± 0.17 (-0.69)
C_β	100 K DNP	-7.0 ± 4.2 (-4.5)	101.2 ± 6.0 (81.7)	0.82 ± 0.18 (-0.03)
C_α	Room Temp	102.9 ± 4.6	185.4 ± 6.5	-1.00 ± 0.11
C_β	Room Temp	-2.8 ± 1.6	126.8 ± 2.3	0.82 ± 0.06

*DFT calculated values are in parenthesis. The functional/basis set used was B3LYP/TZP corrected for spin-orbit coupling (details are given in SI).

By acquiring a CPMAS spectrum at a relatively slow MAS frequency (5.8 kHz), we were able to identify the spinning sidebands associated with the C_α and C_β resonances and measure the chemical

shift anisotropy (CSA) parameters of **TBP-1** (Figure S4a). Deconvolution of the spectrum (Figure S4b-d) allowed us to extract the CSA parameters of each carbon (Table 1). The results compare well with those obtained from room temperature MAS NMR for both C_α and C_β and with DFT calculated CSA parameters corrected for spin orbit coupling in the isotropic shift (δ_{iso}) and span (Ω), which are summarized in Table 1.

Turning to catalyst **2,** (≡SiO)W(NAr)(=CH*t*Bu)(O*t*Bu), treatment with ^{13}C,^{2}H labeled ethylene leads only to 0.2 equiv. of 3,3-dimethyl-2-butene (the cross metathesis product) under the same reaction conditions, indicating slow initiation. Recording DNP SENS under the same conditions (addition of 16 mM TEKPOL[20] polarization agent in TCE) shows an overall signal enhancement of 70 on the 400 MHz spectrometer (Figure S6), possibly due to the presence of the three methyl groups from the O*t*Bu group in the ligand.[15d, 26] The two main peaks in the ^{13}C CPMAS spectrum (shown on the top of Figure 3a) can be tentatively assigned to the C_α and C_β of an SP metallacycle, respectively, by comparison with similar molecular species. The 2D refocused INADEQUATE spectrum confirms this hypothesis with a main correlation observed at 42 and 20 ppm in the single-quantum dimension, and therefore the assignment of these peaks to C_α and C_β of a SP-metallacycle. However, the 2D spectrum also reveals unexpected features, in particular the presence of correlations between two carbons at 47 and 31 ppm, which appears consistent with a SP metallacycle connected to a tertiary butyl group (Figure 3a).[12b]

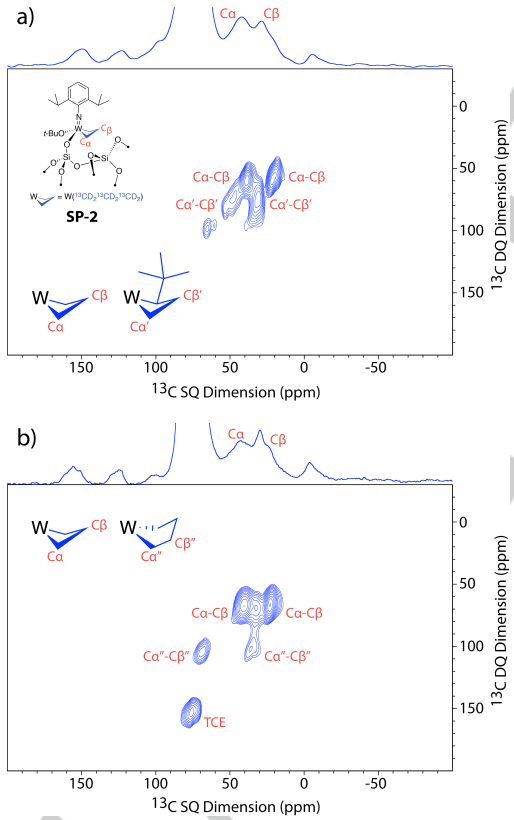

Figure 3. 2D DNP SENS refocused INADEQUATE of a) **SP-2** obtained by reacting **2** with 10 equiv. of labelled ethylene, resulting in the presence of both **SP-2** and a tertiary butyl substituted minor species, and b) **SP-2** obtained by exposing **2** to a large excess of ethylene, yielding **SP-2** and possibly metallacyclopentane.

We reasoned that the observation of this intermediate metallacycle was probably due to the slow initiation of the metathesis process (Scheme 1). In order to favor the formation of the parent metallacyclobutane, we thus first exposed **2** to a large excess of ethylene (800 equiv.) for 12 h and then to 10 equiv. of ^{13}C, ^{2}H labeled ethylene. The 1D ^{13}C NMR spectrum of the material thus formed presents the same overall features as the previous one, with two main peaks at 42 ppm and 20 ppm that can be assigned to the C_α and C_β of the SP metallacycle (Figure 3b), but the 2D INADEQUATE spectrum no longer contains the previously observed correlations associated with the *t*Bu-substituted metallacycle. This thus confirms the full reaction of the neopentylidene moiety and the formation of the parent metallacyclobutane. However, another set of correlations appears at 69 ppm and 36 ppm (marked as C_α" and C_β" in Figure 3b), which are tentatively assigned to a metallacyclopentane moiety formed by a secondary reaction due to the presence of a large excess of ethylene.[27] To confirm that hypothesis, a suspension of this sample in C_6D_6 (see ESI for details) was contacted with Br_2. ^{13}C NMR (Figure S10) and GC-MS (Figure S11) analysis of the product solution revealed the presence of 1,4-dibromobutane as a minor product. This observation is consistent with the presence of the proposed metallacyclopentane complex as a minor surface species. The 2D POSTC7 spectra of this material show that the correlation for the C_α is inhomogeneously broadened (Figure S7), indicating the existence of a distribution of C_α sites. This distribution of sites is not found for the corresponding TBP isomer, likely because the metallacycle lies far from the surface in that geometry; the N-W-OSi angle and the Si-C_α distance are 175° and 4.0 – 4.1 Å for each C_α, respectively, according to DFT calculations (Figure S3 and coordinate file). In contrast, the SP isomer displays a N-W-OSi angle close to 112° and a Si-C_α distance as close as 3.5 Å, bringing the metallacycle closer to the surface, thereby experiencing more the local environment of the amorphous silica support.

Scheme 1. Initiation mechanism and formation of SP metallacyclobutane and metallacyclopentane from the tungsten neopentylidene.

In addition, the 2D POSTC7 spectra reveal the presence of an additional species that is consistent with a TBP metallacycle (Figure S7) but not observed in the INADEQUATE experiment (Figure 3b). This is most likely due to the lower concentration as well as the relatively small C_α-C_β *J* coupling (13 Hz)[12b, 12c, 28] of the TBP metallacycle. Although complex, this result allows a more detailed understanding of the initiation and deactivation of **2.** It further highlights the benefit of acquiring complementary 2D NMR spectra, as they reveal molecular features that could not be foreseen from 1D CPMAS spectra on 100 % labeled compound. Finally, we further characterized **SP-2** by simulating the POSTC7 DQ curves (Figure S9), which yielded a C_α-C_β distance of 1.49 (± 0.12) Å. While this shorter C_α-C_β distance for the SP metallacycle is consistent with the DFT calculated bond distance and with what is expected for this intermediate,[10c] the precision of the measurement does not allow a clear distinction between the two isomers.

In conclusion, we characterized the TBP and SP metallacycle intermediates of tungsten heterogeneous metathesis catalysts by DNP SENS with details at an unprecedented level, including the

monitoring of the initiation and deactivation of the catalysts, using a combination of 1D and 2D NMR techniques. This approach allows observation of the surface species at the atomic level, including direct determination of C-C connectivities and bond distances in metathesis reaction intermediates.

Keywords: DNP SENS, solid-state NMR, alkene metathesis, DFT calculation, Bond distance

[1] a) P. Cossee, *J. Catal.* **1964**, *3*, 80-88; b) K. Soga, T. Shiono, *Prog. Polym. Sci.* **1997**, *22*, 1503-1546.

[2] M. P. McDaniel, *Adv. Catal.* **2010**, *53*, 123-606.

[3] S. Lwin, I. E. Wachs, *ACS Catal.* **2014**, *4*, 2505-2520.

[4] a) B. M. Weckhuysen, I. E. Wachs, R. A. Schoonheydt, *Chem. Rev.* **1996**, *96*, 3327-3349; b) J. J. H. B. Sattler, J. Ruiz-Martinez, E. Santillan-Jimenez, B. M. Weckhuysen, *Chem. Rev.* **2014**, *114*, 10613-10653.

[5] a) C. Coperet, M. Chabanas, R. Petroff Saint-Arroman, J. M. Basset, *Angew. Chem., Int. Edit.* **2003**, *42*, 156-181; b) H. Tada, T. Kiyonaga, S. Naya, *Chem. Soc. Rev.* **2009**, *38*, 1849-1858; c) J. M. Basset, R. Ugo, in *Modern Surface Organometallic Chemistry*, Wiley-VCH Verlag GmbH & Co. KGaA, **2009**, pp. 1-21; d) S. L. Wegener, T. J. Marks, P. C. Stair, *Acc. Chem. Res.* **2012**, *45*, 206-214; e) M. M. Stalzer, M. Delferro, T. J. Marks, *Catal. Lett.* **2015**, *145*, 3-14.

[6] H. P. Jia, E. A. Quadrelli, *Chem. Soc. Rev.* **2014**, *43*, 547-564.

[7] M. D. Christianson, C. R. Landis, *Concept Magn Reson A* **2007**, *30A*, 165-183.

[8] P. S. Pregosin, *NMR in organometallic chemistry*, Wiley-VCH, Weinheim, **2012**.

[9] a) K. J. D. MacKenzie, M. E. Smith, *Multinuclear solid-state NMR of inorganic materials*, 1st ed., Pergamon, Oxford ; New York, **2002**; b) F. Blanc, C. Coperet, A. Lesage, L. Emsley, *Chem. Soc. Rev.* **2008**, *37*, 518-526.

[10] a) X. Solans-Monfort, E. Clot, C. Coperet, O. Eisenstein, *J. Am. Chem. Soc.* **2005**, *127*, 14015-14025; b) A. Poater, X. Solans-Monfort, E. Clot, C. Coperet, O. Eisenstein, *J. Am. Chem. Soc.* **2007**, *129*, 8207-8216; c) X. Solans-Monfort, C. Coperet, O. Eisenstein, *Organometallics* **2015**, *34*, 1668-1680.

[11] V. Mougel, C. Coperet, *Chem. Sci.* **2014**, *5*, 2475-2481.

[12] a) R. R. Schrock, R. T. Depue, J. Feldman, C. J. Schaverien, J. C. Dewan, A. H. Liu, *J. Am. Chem. Soc.* **1988**, *110*, 1423-1435; b) J. Feldman, W. M. Davis, R. R. Schrock, *Organometallics* **1989**, *8*, 2266-2268; c) J. Feldman, W. M. Davis, J. K. Thomas, R. R. Schrock, *Organometallics* **1990**, *9*, 2535-2548.

[13] a) F. Blanc, R. Berthoud, C. Coperet, A. Lesage, L. Emsley, R. Singh, T. Kreickmann, R. R. Schrock, *P. Natl. Acad. Sci. USA* **2008**, *105*, 12123-12127; b) M. P. Conley, W. P. Forrest, V. Mougel, C. Coperet, R. R. Schrock, *Angew. Chem., Int. Edit.* **2014**, *53*, 14221-14224.

[14] a) L. R. Becerra, G. J. Gerfen, B. F. Bellew, J. A. Bryant, D. A. Hall, S. J. Inati, R. T. Weber, S. Un, T. F. Prisner, A. E. Mcdermott, et al., *J. Magn. Reson., Ser. A* **1995**, *117*, 28-40; b) T. Maly, G. T. Debelouchina, V. S. Bajaj, K. N. Hu, C. G. Joo, M. L. Mak-Jurkauskas, J. R. Sirigiri, P. C. A. van der Wel, J. Herzfeld, R. J. Temkin, et al., *J. Chem. Phys.* **2008**, *128*, 052211.

[15] a) A. Lesage, M. Lelli, D. Gajan, M. A. Caporini, V. Vitzthum, P. Mieville, J. Alauzun, A. Roussey, C. Thieuleux, A. Mehdi, et al., *J. Am. Chem. Soc.* **2010**, *132*, 15459-15461; b) D. Lee, H. Takahashi, A. S. L. Thankamony, J. P. Dacquin, M. Bardet, O. Lafon, G. De Paepe, *J. Am. Chem. Soc.* **2012**, *134*, 18491-18494; c) A. J. Rossini, A. Zagdoun, M. Lelli, A. Lesage, C. Coperet, L. Emsley, *Acc. Chem. Res.* **2013**, *46*, 1942-1951; d) A. Zagdoun, A. J. Rossini, M. P. Conley, W. R. Gruning, M. Schwarzwalder, M. Lelli, W. T. Franks, H. Oschkinat, C. Coperet, L. Emsley, et al., *Angew. Chem., Int. Edit.* **2013**, *52*, 1222-1225.

[16] T. Kobayashi, F. d. r. A. Perras, I. I. Slowing, A. D. Sadow, M. Pruski, *ACS Catal.* **2015**, 7055-7062.

[17] a) M. P. Conley, R. M. Drost, M. Baffert, D. Gajan, C. Elsevier, W. T. Franks, H. Oschkinat, L. Veyre, A. Zagdoun, A. Rossini, et al., *Chem. - Eur. J.* **2013**, *19*, 12234-12238; b) T. Gutmann, J. Q. Liu, N. Rothermel, Y. P. Xu, E. Jaumann, M. Werner, H. Breitzke, S. T. Sigurdsson, G. Buntkowsky, *Chem. - Eur. J.* **2015**, *21*, 3798-3805.

[18] a) W. R. Gunther, V. K. Michaelis, M. A. Caporini, R. G. Griffin, Y. Roman-Leshkov, *J. Am. Chem. Soc.* **2014**, *136*, 6219-6222; b) P. Wolf, M. Valla, A. J. Rossini, A. Comas-Vives, F. Nunez-Zarur, B. Malaman, A. Lesage, L. Emsley, C. Coperet, I. Hermans, *Angew. Chem., Int. Edit.* **2014**, *53*, 10179-10183.

[19] a) M. Lelli, D. Gajan, A. Lesage, M. A. Caporini, V. Vitzthum, P. Mieville, F. Heroguel, F. Rascon, A. Roussey, C. Thieuleux, et al., *J. Am. Chem. Soc.* **2011**, *133*, 2104-2107; b) V. Vitzthum, P. Mieville, D. Carnevale, M. A. Caporini, D. Gajan, C. Coperet, M. Lelli, A. Zagdoun, A. J. Rossini, A. Lesage, et al., *Chem. Commun.* **2012**, *48*, 1988-1990; c) O. Lafon, A. S. L. Thankamony, M. Rosay, F. Aussenac, X. Y. Lu, J. Trebosc, V. Bout-Roumazeilles, H. Vezine, J. P. Amoureux, *Chem. Commun.* **2013**, *49*, 2864-2866; d) U. Akbey, B. Altin, A. Linden, S. Ozcelik, M. Gradzielski, H. Oschkinat, *Phys. Chem. Chem. Phys.* **2013**, *15*, 20706-20716; e) D. Lee, G. Monin, N. T. Duong, I. Z. Lopez, M. Bardet, V. Mareau, L. Gonon, G. De Paepe, *J. Am. Chem. Soc.* **2014**, *136*, 13781-13788; f) L. Protesescu, A. J. Rossini, D. Kriegner, M. Valla, A. de Kergommeaux, M. Walter, K. V. Kravchyk, M. Nachtegaal, J. Stangl, B. Malaman, et al., *Acs Nano* **2014**, *8*, 2639-2648; g) L. Piveteau, T.-C. Ong, A. J. Rossini, L. Emsley, C. Coperet, M. V. Kovalenko, *J. Am. Chem. Soc.* **2015**, *137*, 13964-13971.

[20] A. Zagdoun, G. Casano, O. Ouari, M. Schwarzwalder, A. J. Rossini, F. Aussenac, M. Yulikov, G. Jeschke, C. Coperet, A. Lesage, et al., *J. Am. Chem. Soc.* **2013**, *135*, 12790-12797.

[21] A. Lesage, M. Bardet, L. Emsley, *J. Am. Chem. Soc.* **1999**, *121*, 10987-10993.

[22] M. Hohwy, H. J. Jakobsen, M. Eden, M. H. Levitt, N. C. Nielsen, *J. Chem. Phys.* **1998**, *108*, 2686-2694.

[23] a) P. R. Costa, Massachusetts Institute of Technology (Cambridge, MA), **1996**; b) M. J. Bayro, M. Huber, R. Ramachandran, T. C. Davenport, B. H. Meier, M. Ernst, R. G. Griffin, *J. Chem. Phys.* **2009**, *130*; c) G. De Paepe, *Annu. Rev. Phys. Chem.* **2012**, *63*, 661-684.

[24] a) M. Carravetta, M. Eden, O. G. Johannessen, H. Luthman, P. J. E. Verdegem, J. Lugtenburg, A. Sebald, M. H. Levitt, *J. Am. Chem.*

Soc. **2001**, *123*, 10628-10638; b) J. Schmedt auf der Günne, *J. Magn. Reson.* **2003**, *165*, 18-32; c) S. Olejniczak, P. Napora, J. Gajda, W. Ciesielski, M. J. Potrzebowski, *Solid State Nucl. Mag.* **2006**, *30*, 141-149.

[25] M. Bak, J. T. Rasmussen, N. C. Nielsen, *J. Magn. Reson.* **2000**, *147*, 296-330.

[26] M. Rosay, A. C. Zeri, N. S. Astrof, S. J. Opella, J. Herzfeld, R. G. Griffin, *J. Am. Chem. Soc.* **2001**, *123*, 1010-1011.

[27] a) S. Y. S. Wang, D. D. VanderLende, K. A. Abboud, J. M. Boncella, *Organometallics* **1998**, *17*, 2628-2635; b) W. C. P. Tsang, K. C. Hultzsch, J. B. Alexander, P. J. Bonitatebus, R. R. Schrock, A. H. Hoveyda, *J. Am. Chem. Soc.* **2003**, *125*, 2652-2666; c) A. M. Leduc, A. Salameh, D. Soulivong, M. Chabanas, J. M. Basset, C. Coperet, X. Solans-Monfort, E. Clot, O. Eisenstein, V. P. W. Bohm, et al., *J. Am. Chem. Soc.* **2008**, *130*, 6288-6297; d) X. Solans-Monfort, C. Coperet, O. Eisenstein, *J. Am. Chem. Soc.* **2010**, *132*, 7750-7757.

[28] A. J. Jiang, J. H. Simpson, P. Muller, R. R. Schrock, *J. Am. Chem. Soc.* **2009**, *131*, 7770-7780.

[29] M. Carravetta, X. Zhao, O. G. Johannessen, W. C. Lai, M. A. Verhoeven, P. H. M. Bovee-Geurts, P. J. E. Verdegem, S. Kiihne, H. Luthman, H. J. M. de Groot, et al., *J. Am. Chem. Soc.* **2004**, *126*, 3948-3953.

[30] a) J. J. Wittmann, K. Takeda, B. H. Meier, M. Ernst, *Angew. Chem., Int. Edit.* **2015**, *54*, 12592-12596; b) J. J. Wittmann, V. Mertens, K. Takeda, B. H. Meier, M. Ernst, *J. Magn. Reson.* **2016**, *263*, 7-18.

Entry for the Table of Contents

COMMUNICATION

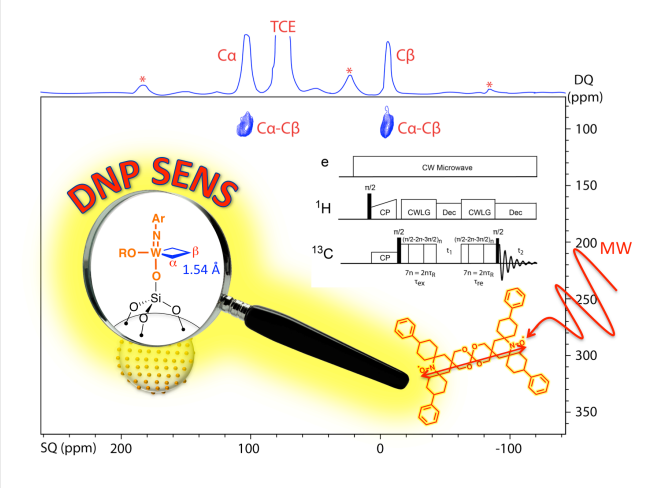

*Ta-Chung Ong, Wei-Chih Liao, Victor Mougel, David Gajan, Anne Lesage, Lyndon Emsley, Christophe Copéret**

1 – 4

Atomistic Description of Reaction Intermediates in Supported Heterogeneous Metathesis Catalysts enabled by DNP SENS

SENSing the structure: We use dynamic nuclear polarization surface enhanced solid-state NMR spectroscopy (DNP SENS) to investigate the catalytic intermediates of a well-defined tungsten alkylidene metathesis catalyst, present in low concentration at the surface of the silica support material. The increase in NMR signal sensitivity allows establishing C-C connectivity and distance measurement via a combination of 1D and 2D NMR techniques on a minute amount of surface sites.

Table of Contents **Page Number**

Materials. Compounds (≡SiO)W(NAr)(=CH*t*Bu)(O*t*Bu), (≡SiO)W(NAr)(=CH*t*Bu)(O*t*Bu$_{F9}$) and (≡SiO)W(NAr)($^{13}CH_2{}^{13}CH_2{}^{13}CH_2$)(O*t*Bu$_{F9}$) were synthesized according to literature procedures.[1]

Synthesis of TBP and SP metallacyclebutanes.

Synthesis of (≡SiO)W(NAr)($^{13}CD_2{}^{13}CD_2{}^{13}CD_2$)(O*t*Bu$_{F9}$): 100 mg of (≡SiO)W(NAr)(=CH*t*Bu)(O*t*Bu$_{F9}$) (18.9 μmol, 1 equiv.) was loaded in a glass reactor and evacuated under high vacuum (10^{-5} mBar). 284 μmol of ^{13}C dilabeled perdeuterated ethylene (15 equiv.) were vacuum transferred on the grafted complex at -196 °C. After standing 1h at room temperature, the volatiles were vacuum transferred and the solid was dried under high vacuum (10^{-5} mbar) at room temperature for 1h30, and stored at -40 °C.

Synthesis of (≡SiO)W(NAr)($^{13}CD_2{}^{13}CD_2{}^{13}CD_2$)(O*t*Bu): 100 mg of (≡SiO)W(NAr)(=CH*t*Bu)(O*t*Bu) (18 μmol, 1 equiv.) was loaded in a glass reactor and evacuated under high vacuum (10^{-5} mBar). 1 atmosphere of ethylene was vacuum transferred on the grafted complex at -196 °C. After standing 2h at room temperature, the volatiles were evacuated and the sample was dried under high vacuum (10^{-5} mbar) at room temperature. This ethylene exposure/evacuation step was repeated twice. 280 μmol of ^{13}C dilabeled perdeuterated ethylene (15.5 equiv.) were vacuum transferred on the grafted complex at -196 °C. After standing 5h at room temperature, the volatiles were vacuum transferred and the solid was dried under high vacuum (10^{-5} mbar) at room temperature for 1h30, and stored at -40 °C.

DNP sample preparation. The radical solution used for the DNP polarization experiments consists of 16 mM TEKPol in 1,1,2,2-tetrachloroethane (TCE). In order to remove possible water residue, the solid TEKPol sample was dried under high vacuum (10^{-4} mbar) at room temperature for 4 hours, and TCE was stirred over calcium hydride under argon for 1 day and distilled *in vacuo*. For experiments that benefit from longer T_2', a reduced concentration of 4 mM TEKPol in TCE was used. Incipient wetness impregnation was used to deliver the radical solution to the solid powder at a ratio of 1 μL per mg. All rotors were packed inside an argon atmosphere glove box. The packed sample was then immediately inserted into the pre-cooled DNP probe for experiments.

NMR pulse sequences.

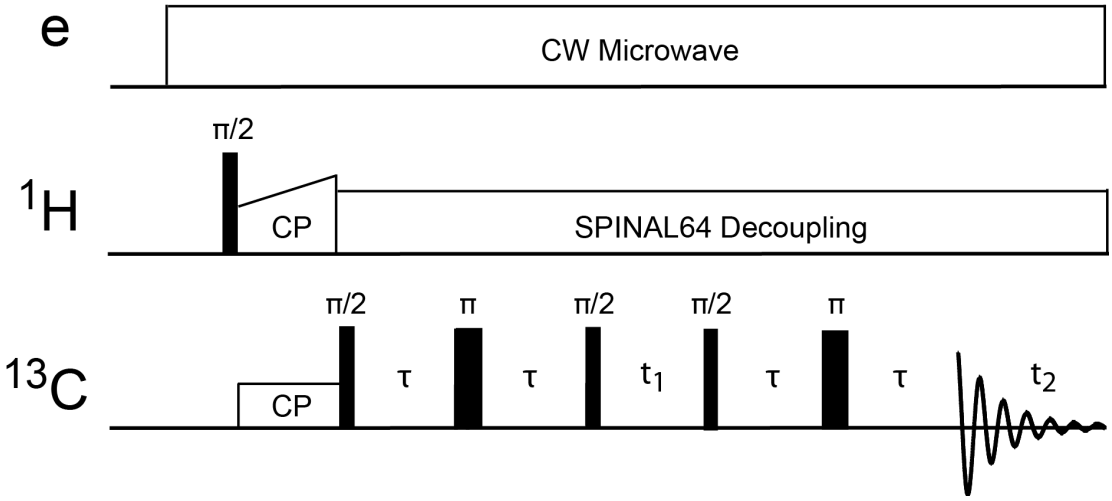

Figure S1. DNP enhanced refocused INADEQUATE. τ is synchronized to be an integer number of rotor periods.

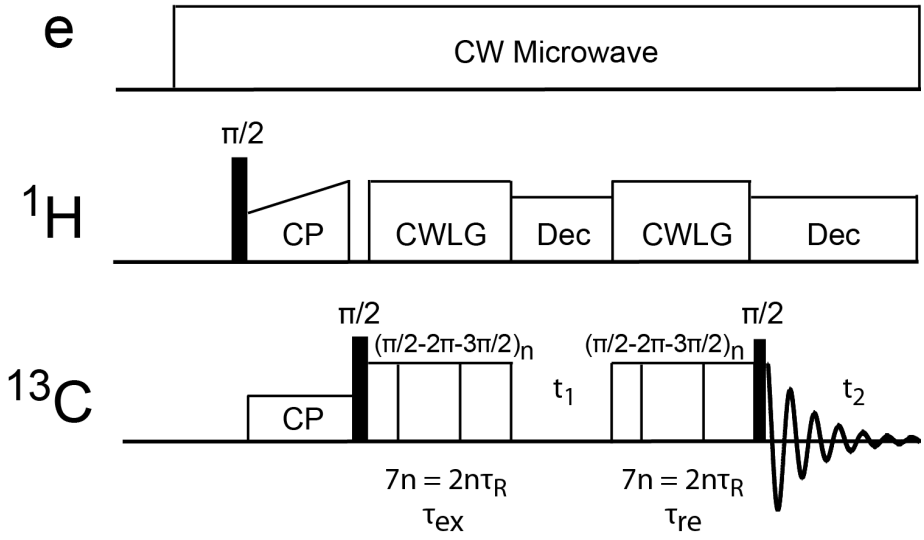

Figure S2. DNP enhanced POSTC7. Continuous-wave Lee Goldburg decoupling is applied during the C7 periods (CWLG), and SPINAL64 is used during t_1 and t_2 periods (Dec).

DNP enhanced solid-state NMR. DNP enhanced solid-state NMR experiments were conducted on a 600 MHz (14.1 T) spectrometer (Bruker Biospin) using a 3.2 mm HX or HXY probe located at ETH Zurich, and on a 400 MHz (9.4 T) spectrometer[2] (Bruker Biospin) using a 3.2 mm HXY probe located at the Centre de RMN à Trés Hauts Champs at CNRS Lyon. The sample is cooled to 100 K by a cryogenic heat exchanger system. Microwaves used to generate electron polarization are provided by gyrotrons emitting at 263 GHz (400 MHz spectrometer) and 395 GHz (600 MHz spectrometer) with power between 6 to 10 W. Ramped cross polarization (CP)[3] from ^{1}H to heteronuclei was used for all experiments with contact time between 0.5 to 2.0 ms. Unless otherwise noted, SPINAL64[4] was used for ^{1}H decoupling at γB_1 of 100 kHz. The DNP build up time (T_B) was measured by saturation recovery,[5] and the recycling delay time was set to 1.3xT_B. All ^{13}C DNP NMR spectra were referenced to adamantane with the higher frequency peak set to 38.48 ppm with respect to TMS (0 ppm).[6] Potassium bromide (KBr) was used to calibrate the magic angle for the MAS probes.

The DNP enhanced 2D POSTC7[7] spectrum was acquired at 400 MHz with magic angle spinning (MAS) frequency of 8 kHz. Continuous-wave Lee-Goldburg (CWLG)[8] ^{1}H decoupling was used during C7 excitation and reconversion blocks. The number of t_1 increment was 512, and the number of scans for each increment was 16. The number of full C7 blocks for excitation and reconversion was 3 each. Distance measurement[9] by DNP enhanced 1D POSTC7 between C_α and C_β was acquired at 600 MHz with MAS frequency of 7 kHz for the TBP metallacycle. For the SP metallacycle, the experiment was acquired at 400 MHz with MAS frequency of 8 kHz to take advantage of the higher enhancement

available there. As with the 2D experiment, CWLG was applied during C7 blocks. For the symmetric procedure, τ_{ex} and τ_{re} were incremented in the same way so that τ_{ex} equals τ_{re}. For the constant time procedure, τ_{ex} is incremented while τ_{re} is reduced so that $\tau_{ex}+\tau_{re}$ remains constant. The total number of full C7 blocks for the constant time procedure was 14. Simulation of POSTC7 DQ efficiency was conducted using SIMPSON[10] to obtain the homonuclear dipolar coupling ($b/2\pi$) and the distance between two ^{13}C spins.

The DNP enhanced 2D refocused INADEQUATE[11] experiments were acquired at 400 MHz with MAS frequency of 8 kHz. A mixing time of 2 ms was used for both the TBP and the SP metallacycle. The number of t_1 increments was 192 for the TBP and 64 for the SP. The number of scans for each increment was 64 for the TBP and 512 for the SP.

We found that deuteration of the TBP and SP metallacycle increases ^{13}C T_2'. At 16 mM TEKPol concentration, the ^{13}C transverse relaxation time constant (T_2') of C_α is 6.1 ms and for C_β the T_2' is 5.5 ms for the deuterated TBP metallacycle, both values are longer than the T_2' of the protonated TCE, which is 1.9 ms. For the deuterated SP metallacycle, at 16 mM TEKPol concentration the T_2' for both carbon resonances are 5.8 ms, similar to that observed for the TBP metallacycle.

DFT calculations. Structural optimization was carried out using Gaussian09 software[12] with B3PW91 functional[13] and 6-31G(*d*,*p*) basis sets for H, C, N, O, and F. SDD pseudo-potential was used for Si and W with additional polarization function (*d* and *f*, for Si and W, respectively). NMR parameters calculations taking into account spin-orbit coupling were carried out using the Amsterdam Density Functional (ADF) program[14] with B3LYP functional[13a, 15] and TZP basis sets for all elements. GaussView[16] is used to visualize the optimized structures. Calculated chemical shifts were obtained using σ_{ref} of 185.21 ppm (TMS).

Optimized structures.

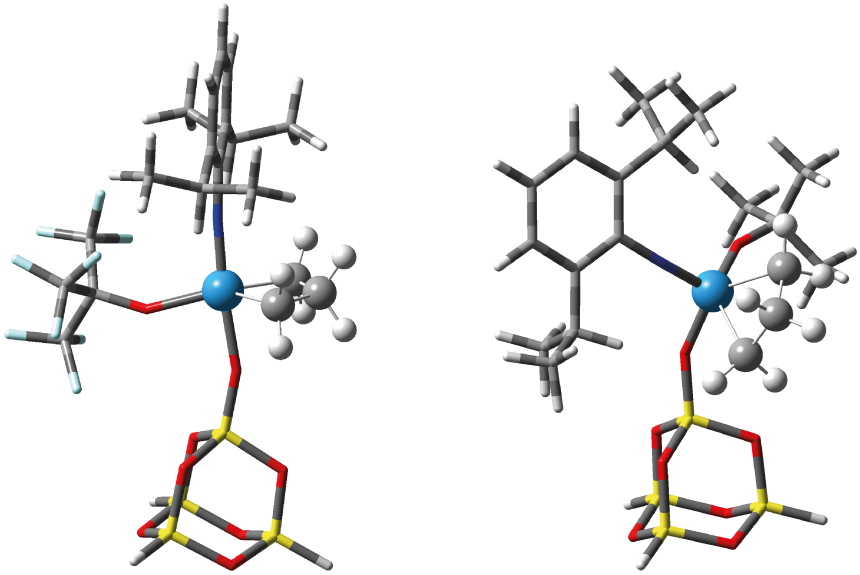

Figure S3. Optimized structures of (left) the TBP metallacycle **(TBP-1)** with the formula (≡SiO)W(NAr)($CH_2CH_2CH_2$)(O*t*Bu_{F9}), and (right) the SP metallacycle **(SP-2)** with the formula (≡SiO)W(NAr)($CH_2CH_2CH_2$)(O*t*Bu). The color scheme is as follows: C: dark gray, H: light gray, W: blue, O: red, Si: yellow, N: dark blue, F: cyan.

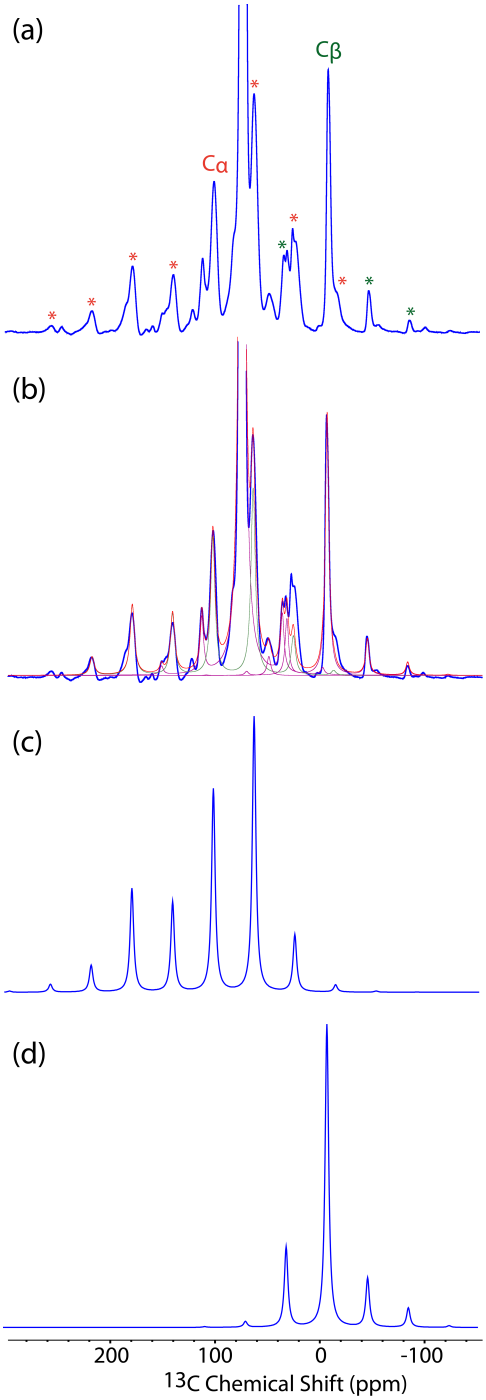

Figure S4. DNP enhanced ^{13}C CPMAS spectrum of the TBP metallacycle (**TBP-1**) at lower MAS frequency (5.8 kHz), a) the experimental spectrum acquired at a 600 MHz spectrometer, b) the experimental spectrum deconvoluted using Bruker's Topspin program, the extracted CSA parameters are listed in Table S1, c) simulated spectrum of C_α, and d) simulated spectrum of C_β obtained using WSolids.[17]

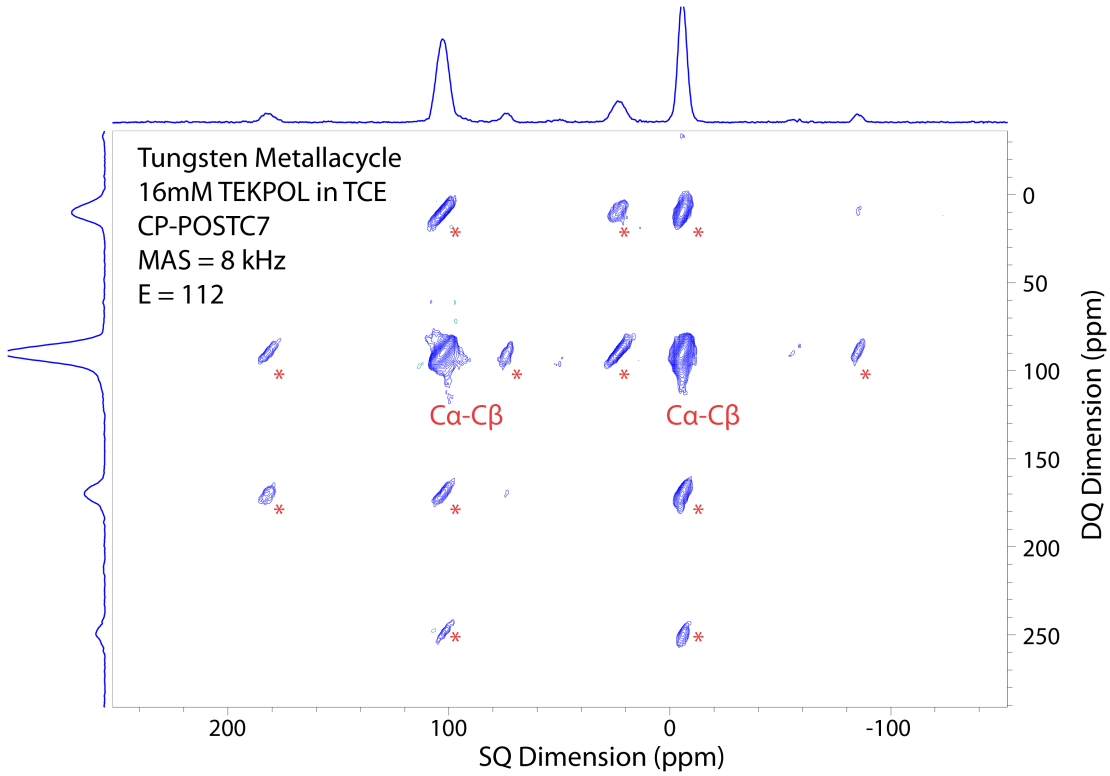

Figure S5. DNP enhanced ^{13}C 2D POSTC7 of the TBP tungsten metallacycle (**TBP-1**). While the C_α-C_β correlations were readily observed, the C_α-C_α correlation was not observed most likely due to the effect of dipolar truncation. Spinning sidebands are denoted with an asterisk.

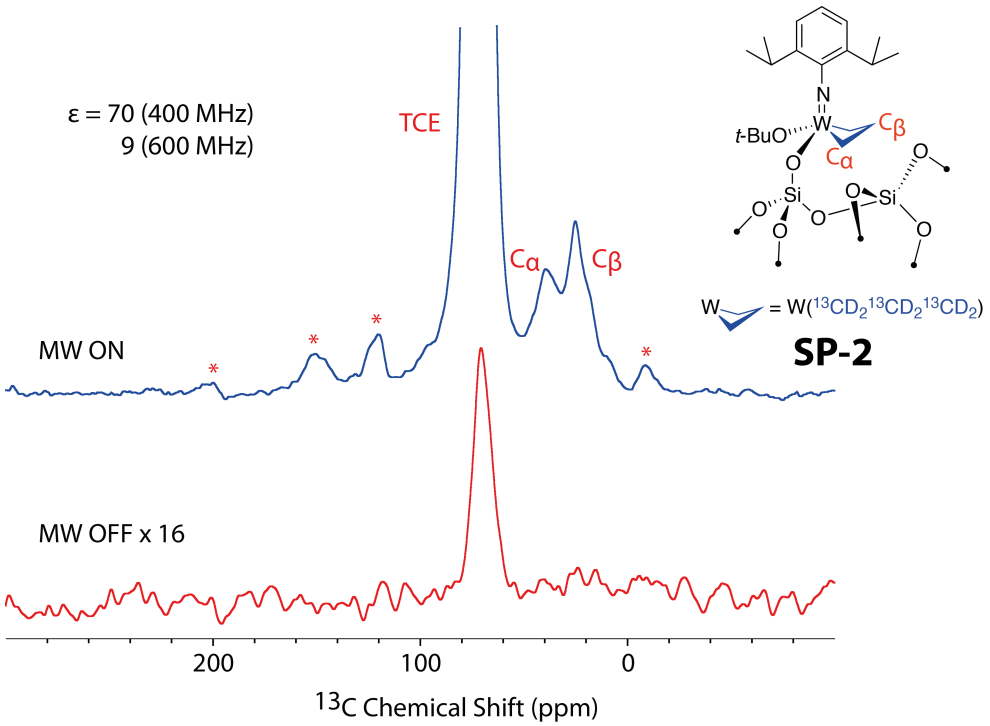

Figure S6. ^{13}C CPMAS DNP enhanced spectrum of ^{13}C and ^{2}H labeled tungsten SP metallacycle (**SP-2**) in 16 mM TEKPol in TCE acquired at the 400 MHz DNP enhanced NMR spectrometer.

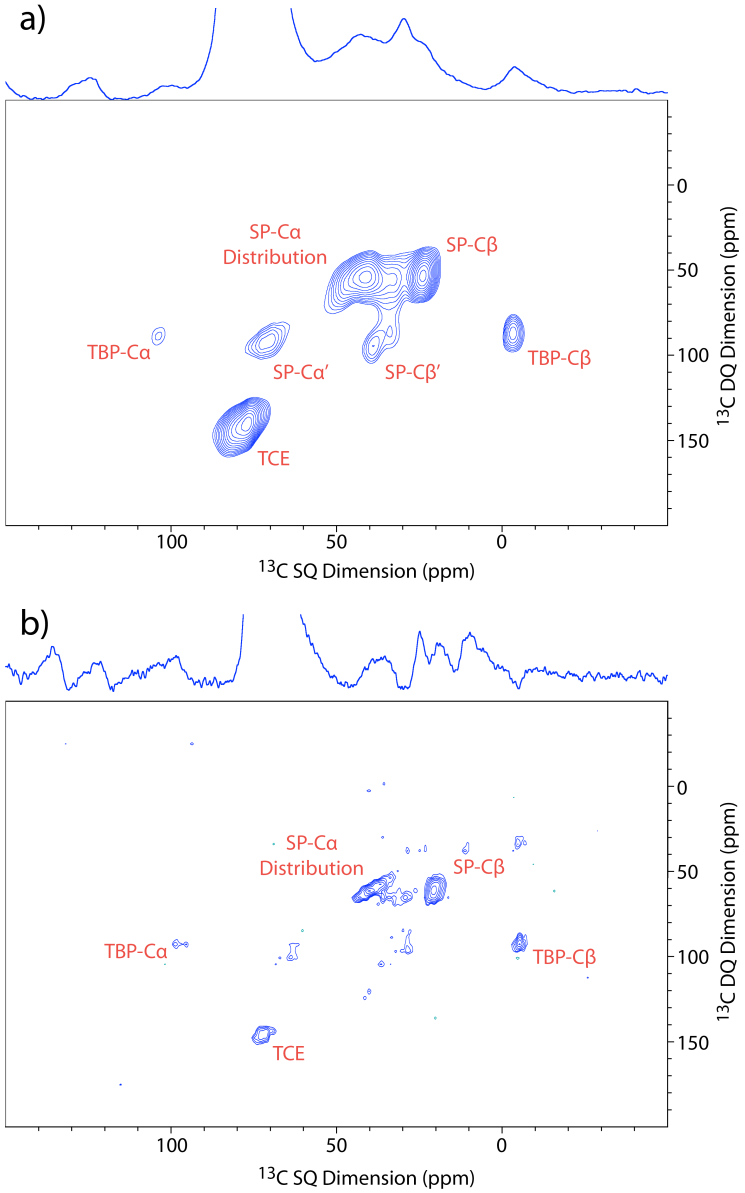

Figure S7. DNP enhanced ^{13}C 2D POSTC7 of the SP tungsten metallacycle acquired at a) 400 MHz and b) 600 MHz. The SP C_α resonance is heterogeneously broadened, indicating that there is a distribution of C_α sites stemming from structural irregularity. As with the case of the TBP metallacycle, the C_α-C_α DQ is not observed due to the effect of dipolar truncation.

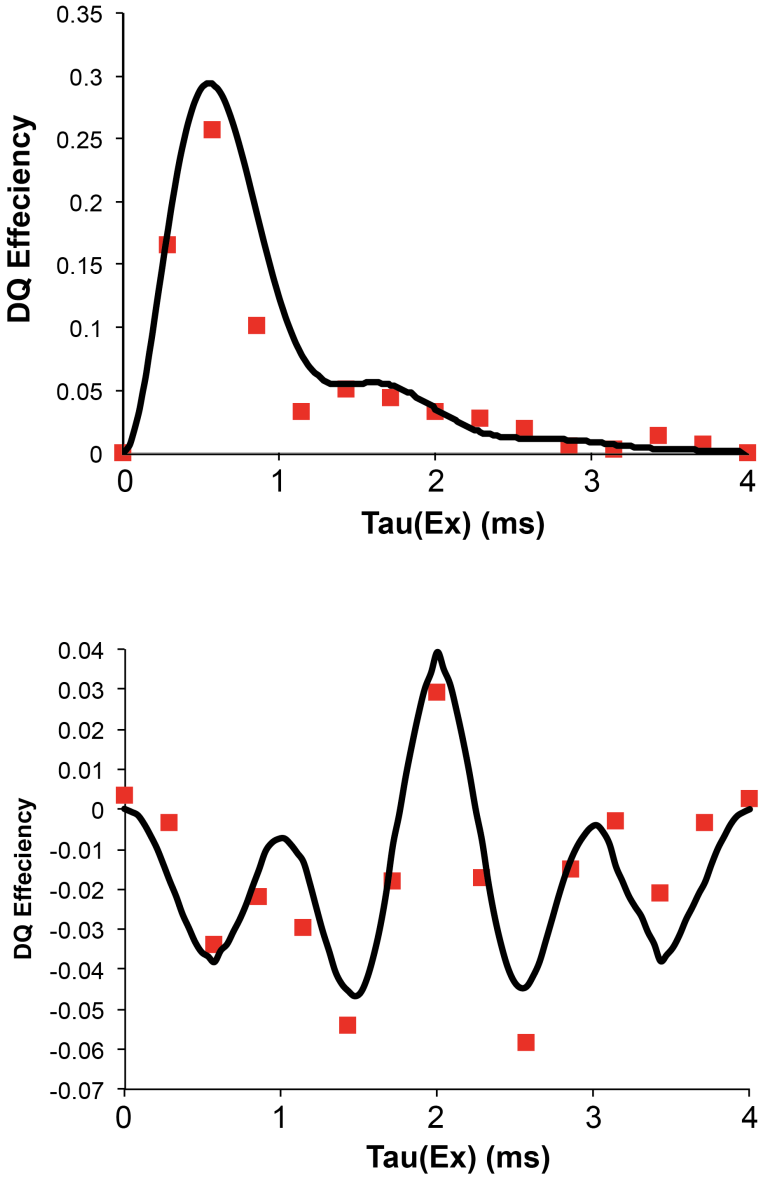

Figure S8. ^{13}C POSTC7 DQ efficiency measured by a) the symmetric procedure, and b) the constant time procedure for the TBP metallacycle. The red squares are experimental data points and the black solid line is simulation with dipolar coupling $b/2\pi$ of -2100 Hz, which corresponds to ^{13}C-^{13}C internuclear distance of 1.54 Å. For the symmetric procedure, an exponential decay term was added to the simulation to capture the effect of transverse relaxation. MAS frequency was 7 kHz, and ^{13}C γB_1 was 49 kHz.

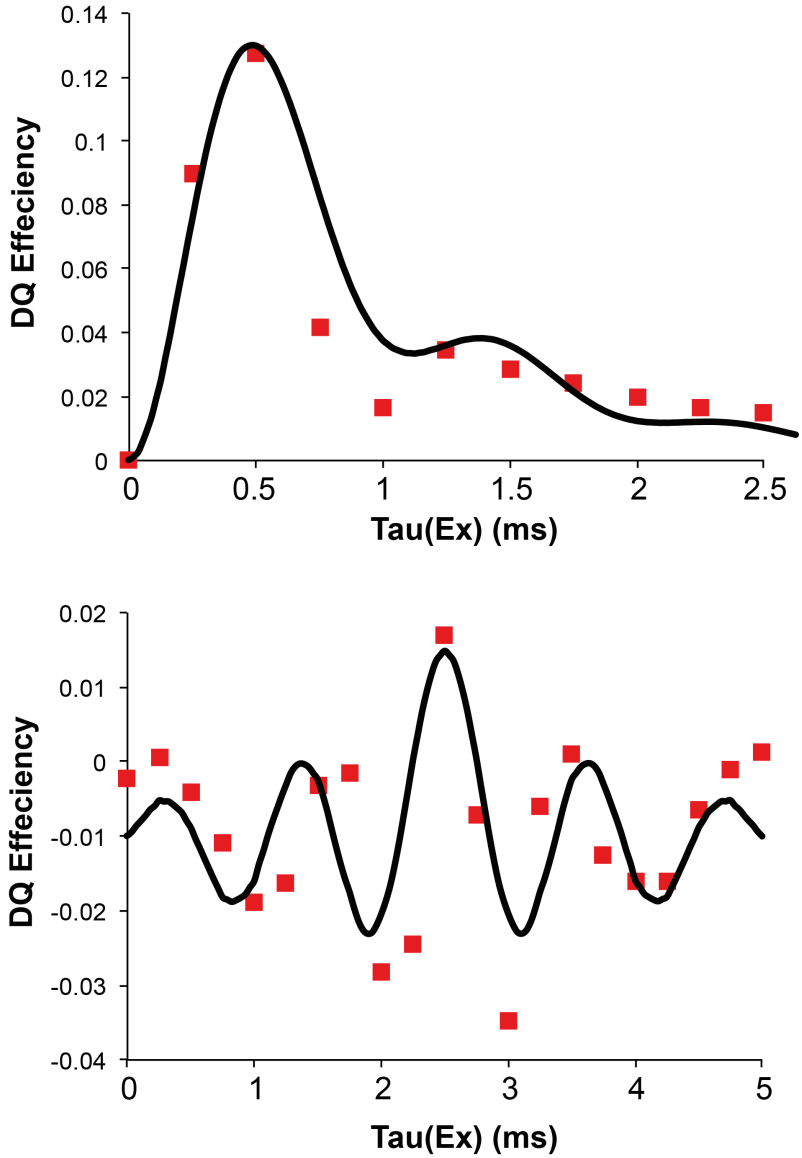

Figure S9. ^{13}C POSTC7 DQ efficiency measured by a) the symmetric procedure, and b) the constant time procedure for the SP metallacycle. The red squares are experimental data points and the black solid line is simulation with dipolar coupling $b/2\pi$ of -2300 Hz, which corresponds to ^{13}C-^{13}C internuclear distance of 1.49 Å. For the symmetric procedure, an exponential decay term was added to the simulation to capture the effect of transverse relaxation. For the constant time simulation, a DQ efficiency offset of -0.01 was added. MAS frequency was 8 kHz, and ^{13}C γB_1 was 56 kHz.

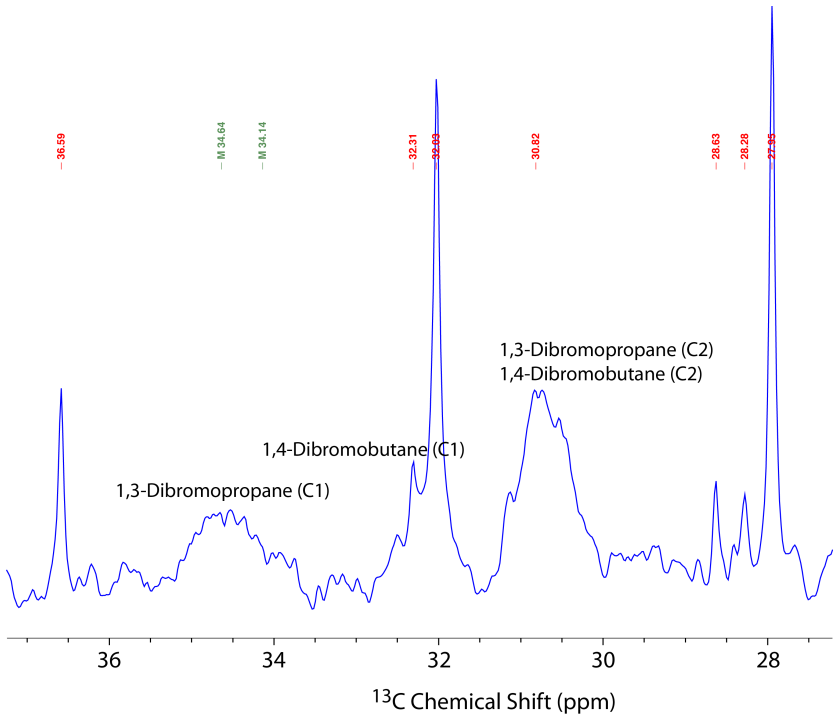

Figure S10. ^{13}C solution NMR spectrum of 1,3-dibromopropane and 1,4-dibromobutane after reaction of the SP metallacycle sample with Br_2 in deuterated benzene (C_6D_6). The presence of 1,4-dibromobutane indicates that a trace amount of metallacyclopentane was formed in the SP metallacycle sample. The spectrum was acquired at a 500 MHz solution NMR spectrometer.

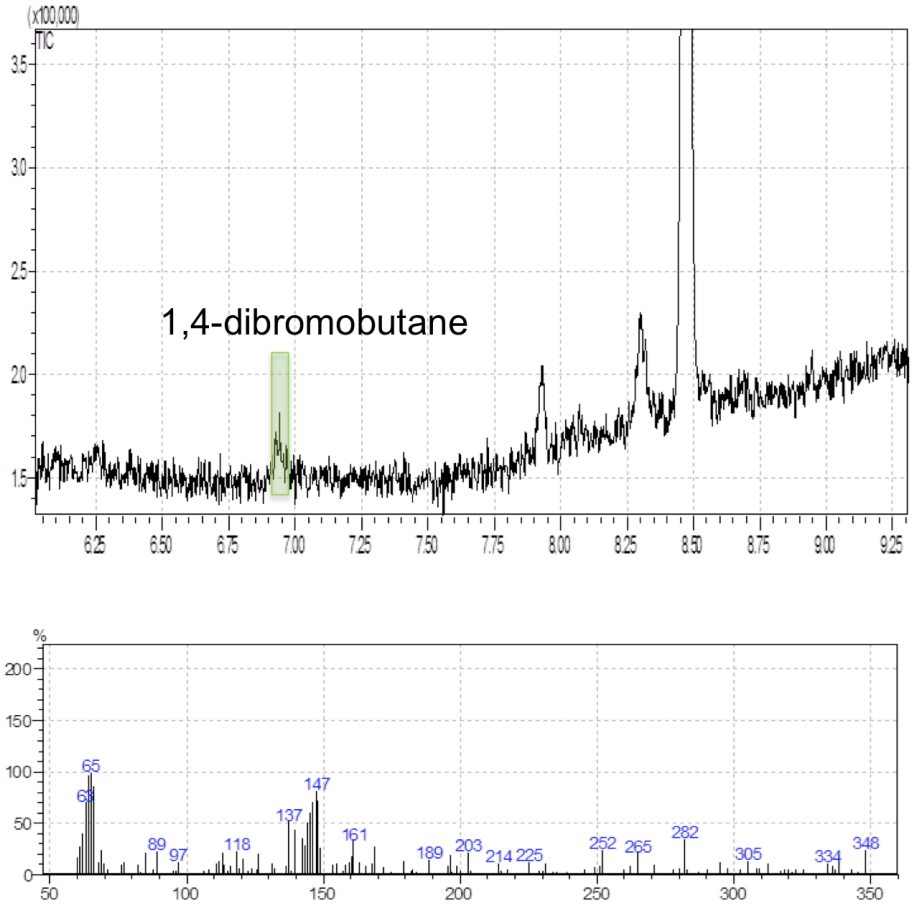

Figure S11. GC-MS of the reaction mixture after reaction of the SP metallacycle sample with excess Br_2 in C_6D_6. From external calibration, retention time for 1,4-dibromobutane was determined to be equal to 6.95 min. MS data of the peak at this retention time confirms the presence of ^{13}C, ^{2}H labeled 1,4-dibromobutane from ^{13}C, ^{2}H labeled metallacyclepentane.

References

[1] V. Mougel, C. Coperet, *Chem. Sci.* **2014**, *5*, 2475-2481.

[2] M. Rosay, L. Tometich, S. Pawsey, R. Bader, R. Schauwecker, M. Blank, P. M. Borchard, S. R. Cauffman, K. L. Felch, R. T. Weber, R. J. Temkin, R. G. Griffin, W. E. Maas, *Phys. Chem. Chem. Phys.* **2010**, *12*, 5850-5860.

[3] aA. Pines, J. S. Waugh, M. G. Gibby, *J. Chem. Phys.* **1972**, *56*, 1776-1777; bG. Metz, X. L. Wu, S. O. Smith, *J. Magn. Reson., Ser. A* **1994**, *110*, 219-227.

[4] B. M. Fung, A. K. Khitrin, K. Ermolaev, *J. Magn. Reson.* **2000**, *142*, 97-101.

[5] R. Freeman, H. D. W. Hill, *J. Chem. Phys.* **1971**, *54*, 3367-3377.

[6] C. R. Morcombe, K. W. Zilm, *J. Magn. Reson.* **2003**, *162*, 479-486.

[7] M. Hohwy, H. J. Jakobsen, M. Eden, M. H. Levitt, N. C. Nielsen, *J. Chem. Phys.* **1998**, *108*, 2686-2694.

[8] aV. Ladizhansky, S. Vega, *J. Chem. Phys.* **2000**, *112*, 7158-7168; bM. Lee, W. I. Goldburg, *Phys Rev* **1965**, *140*, A1261-A1271.

[9] J. Schmedt auf der Günne, *J. Magn. Reson.* **2003**, *165*, 18-32.

[10] M. Bak, J. T. Rasmussen, N. C. Nielsen, *J. Magn. Reson.* **2000**, *147*, 296-330.

[11] A. Lesage, M. Bardet, L. Emsley, *J. Am. Chem. Soc.* **1999**, *121*, 10987-10993.

[12] M. J. Frisch, G. W. Trucks, H. B. Schlegel, G. E. Scuseria, M. A. Robb, J. R. Cheeseman, G. Scalmani, V. Barone, B. Mennucci, G. A. Petersson, H. Nakatsuji, M. Caricato, X. Li, H. P. Hratchian, A. F. Izmaylov, J. Bloino, G. Zheng, J. L. Sonnenberg, M. Hada, M. Ehara, K. Toyota, R. Fukuda, J. Hasegawa, M. Ishida, T. Nakajima, Y. Honda, O. Kitao, H. Nakai, T. Vreven, J. A. Montgomery Jr., J. E. Peralta, F. o. Ogliaro, M. J. Bearpark, J. Heyd, E. N. Brothers, K. N. Kudin, V. N. Staroverov, R. Kobayashi, J. Normand, K. Raghavachari, A. P. Rendell, J. C. Burant, S. S. Iyengar, J. Tomasi, M. Cossi, N. Rega, N. J. Millam, M. Klene, J. E. Knox, J. B. Cross, V. Bakken, C. Adamo, J. Jaramillo, R. Gomperts, R. E. Stratmann, O. Yazyev, A. J. Austin, R. Cammi, C. Pomelli, J. W. Ochterski, R. L. Martin, K. Morokuma, V. G. Zakrzewski, G. A. Voth, P. Salvador, J. J. Dannenberg, S. Dapprich, A. D. Daniels, ñ. n. Farkas, J. B. Foresman, J. V. Ortiz, J. Cioslowski, D. J. Fox, Gaussian, Inc., Wallingford, CT, USA, **2009**.

[13] aA. D. Becke, *J. Chem. Phys.* **1993**, *98*, 5648-5652; bJ. P. Perdew, Y. Wang, *Phys Rev B* **1992**, *45*, 13244-13249.

[14] G. te Velde, F. M. Bickelhaupt, E. J. Baerends, C. F. Guerra, S. J. A. Van Gisbergen, J. G. Snijders, T. Ziegler, *J Comput Chem* **2001**, *22*, 931-967.

[15] C. T. Lee, W. T. Yang, R. G. Parr, *Phys Rev B* **1988**, *37*, 785-789.

[16] R. Dennington, T. Keith, J. Millam, 5 ed., Semichem Inc., Shawnee Mission, KS, **2009**.

[17] K. Eichele, 1.20.21 ed., Universitat Tubingen, **2013**.